

EVALUATION OF THE POTENTIAL OF CENTRAL RECEIVER SOLAR POWER PLANTS: CONFIGURATION, OPTIMIZATION AND TRENDS

Antonio L. Avila-Marin¹, Jesus Fernandez-Reche², Felix M. Tellez³

¹ Plataforma Solar de Almería-CIEMAT, Avda. Complutense 40, Madrid, E-28040, Spain. Email: antonio.avila@ciemat.es

² Plataforma Solar de Almería-CIEMAT, P.O. Box 22, Tabernas-Almeria E-04200, Spain

³ Astrom Technical Advisors, C. Serrano 8, Madrid, Spain.

Abstract

This paper presents a parametric analysis for a medium to large size (290-to-500 MW_{th} receiver thermal power) Central Receiver plant considering the present market trends. The analysis is divided in 4 steps:

- Size and location analysis: for a medium to large size Central Receiver power plant, three turbine power and three different locations that are involved in the development of power tower plants, have been analyzed to assess the impact over the design characteristics of the solar field and receiver sub-systems and over the leveled electricity cost,
- Technology analysis: as commercial power tower plants in operation today are mainly using steam and molten nitrate salts, the present analysis compares the two main technologies, without thermal energy storage to evaluate both under similar design conditions,
- Storage analysis: thermal energy storage increases the value of electricity produced and the plant capacity factor for both technologies (steam and molten nitrate salts). For this reason, the analysis shows for each optimized solar field and receiver thermal power, the optimum combination of turbine power and thermal energy storage that minimizes the leveled electricity cost, for both technologies,
- Component's cost analysis: market trends are focused on the specific cost reduction by means of larger plant size and through an improved economy of scale. As a result, and based on baseline cost parameters widely accepted in solar industry, an analysis over the specific costs of major components on the electricity cost has been carried out, to lead where the research and development efforts should be made.

Keywords: Levelized electricity cost, molten nitrate salts, direct steam generation, steam, thermal energy storage, central receiver.

37	Acronym	
38	BOP	Block of Power
39	CR	Central Receiver
40	DNI	Direct Normal Irradiance
41	DSG	Direct Steam Generation
42	HTF	Heat Transfer Fluid
43	ITD	Initial Temperature Difference
44	LEC	Levelized Electricity Cost
45	MNS	Molten Nitrate Salts
46	NREL	National Renewable Energy Laboratories
47	O&M	Operation and Maintenance
48	PCM	Phase Change Material
49	PSA	Plataforma Solar de Almeria
50	RMS	Root Mean Square
51	SAM	System Advisor Model
52	STE	Solar Thermal Electricity
53	STPP	Solar Thermal Power Plants
54	TES	Thermal Energy Storage
55	TIOS	Total Investment at Operation Startup
56	TMY	Typical Meteorological Year
57		
58	Nomenclature	
59	A	Area
60	C	Cost
61	crf	Fixed charge rate
62	E_{net}	Annual net electricity
63	k_d	Real debt interest rate
64	K_{fuel}	Annual fuel costs
65	$k_{\text{insurance}}$	Annual insurance rate
66	K_{invest}	Total plant investment
67	$K_{\text{O\&M}}$	Annual operation and maintenance costs
68	n	Depreciation period in years
69	P	Gross power rating
70	S	Slant range from heliostat to receiver
71	y	Year
72		
73	Subscript	
74	e	electrical
75	PB	power block
76	rec	receiver
77	ref	reference
78	SG	steam generator
79	th	thermal
80		
81	Superscript	
82	x	scaling exponent
83		
84	Symbol	
85	η	efficiency (design point for power block)

86 τ atmospheric transmittance
87
88

89 **1. Introduction**

90 Solar thermal power plants (STPP) have a great capacity for large-scale electricity
91 generation and the possible combination with thermal energy storage and/or hybridization
92 with backup fossil fuels. These options make possible to supply an important amount of
93 the energy demand in the countries of the solar belt [1]. The first generation of grid-
94 connected power plants for electricity production, based on solar thermal electricity (STE)
95 plants with central receiver (CR) system technology using large heliostat fields and a solar
96 receiver placed on the top of a tower, is currently being boosted by the first commercial
97 plants in Spain, PS10, PS20 and Gemasolar; and in USA, Sierra Sun Tower and Coalinga
98 plant, Ivanpah project, and Tonopah projects which are in the pipeline to start production
99 next years. Nowadays, other countries besides Spain and the USA, are implementing STE
100 projects such as India, China, Israel, Australia, Algeria, South Africa and Italy due to its
101 appropriate solar resource.

102 Present trends are focused on the specific cost reduction by increasing the plant size
103 through an improved economy of scale. On the other hand, the larger plant size the larger
104 optical losses due to atmospheric attenuation and the higher spillages associated to large
105 solar fields with optimized receiver sizes.

106 Moreover, the first generation of commercial STE with CR technology is based on
107 technological developments matured after more than two decades of research, using cavity
108 or external tube receivers with saturated steam and molten salts schemes respectively.
109 Other developments are being implemented with superheated steam, Sierra Sun Tower in
110 USA and Khi Solar One in South Africa, or larger plant sizes, Crescent Dunes (110 MW_e)
111 and Ivanpah Solar Electric Generating Station (377 MW_e) in the USA.

112 As a result of the aforementioned commercial situation, this work presents an analysis over
113 the following factors for a medium to large size CR power plants (between 0.5 to 1.0 km²
114 solar field aperture with 290-to-500 MW_{th} receiver thermal power):

- 115 1. The solar field optical efficiency and relative levelized electricity cost (LEC) for three
116 locations (Seville-Spain, Daggett-USA and Carnarvon-South Africa) due to its relevance
117 in the STE market,
- 118 2. The main implications of the receiver using molten salts and superheated steam as heat
119 transfer fluid,
- 120 3. The impact of different combinations of thermal energy storage and power block sizes
121 for a given reflective surface,
- 122 4. The specific cost of major components (heliostat, receiver, thermal storage, power
123 block, steam generator and operation-maintenance) over the expected LEC.

124 Section 2 presents a detailed description of the four analyses carried out on the paper
125 taking into account the general considerations (modeling, optimization and simulation
126 tools as well as the boundary conditions) introduced on section 3. The methodology used
127 on the simulations and the results of the four cases are presented on section 4. Finally, on
128 section 5, main conclusions of the different analysis are pointed out.

130 **2. Description of the analysis**

131 **2.1. Reference system design**

132 This section describes the STPP configuration that is considered as the reference system
133 for the analysis. It consists on a CR power tower with TES, located next to Seville, Spain.
134 Fig. 1 depicts a schematic view of this reference system. The main sub-systems are the
135 solar field, receiver, TES system, power block, and steam generator.

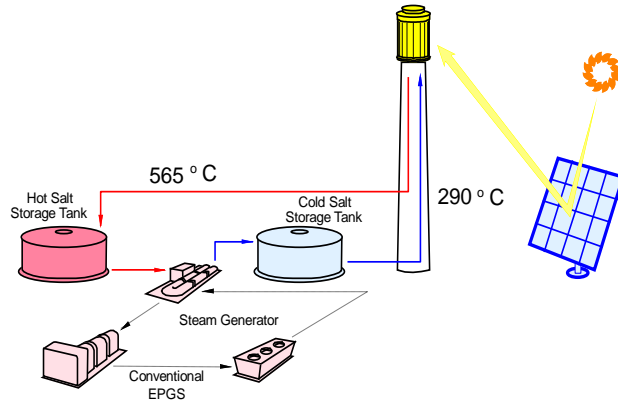


Fig. 1. Scheme of the MNS reference power tower plant

136

137 The HTF in the receiver is MNS, which is heated from 290 °C to 565 °C, and the working
138 fluid in the BOP is steam. The MNS is an eutectic mixture of 60%/40% by weight of
139 sodium/potassium nitrates respectively, called Solar Salt. The thermodynamic cycle is a
140 regenerative Rankine cycle with reheat. The heat exchanger transfer thermal energy from
141 the MNS to the water/steam in the steam generator to run the turbine. The storage is an
142 indirect system [2] that stores salts to work the turbine 15 hours at full load without solar
143 irradiation [3]. The main parameters of the reference plant are presented in Table I.

144 Based on the financing and baseline costs presented on section 3.3. the estimated LEC for
145 the reference plant is 22.442 c€/kWh. Fig. 2 shows the influence of the sub-systems of the
146 reference power plant over the LEC.

147

Table I. Reference plant main parameters

Net aperture, m ²	305,704
Optical tower height, m	140
Receiver thermal power, MW _{th}	120
TES, h	15
Gross output power, MW _e	19.9
Annual energy production, GWh	95

148

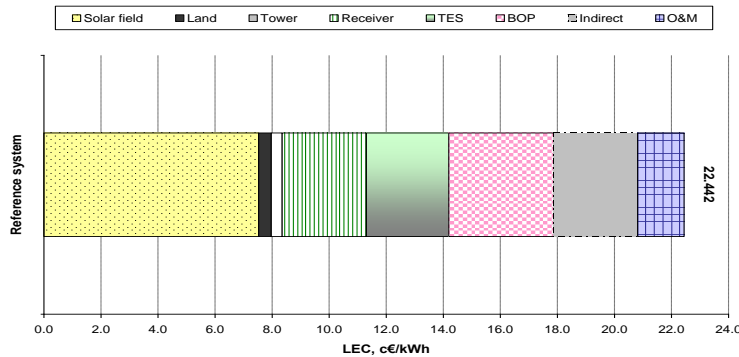


Fig. 2. Influence of the sub-systems of the reference power plant over the LEC

149

150 **2.2. Case I: Size and location analysis**

151 Given the success of the first commercial CR plants, short-medium term designs tend to
 152 increase the plant size with larger solar fields, receivers and power blocks to maximize the
 153 electricity generation and minimize the specific cost of the installation and, consequently
 154 the LEC. Even though there is who still believes that the key to reduce the LEC still lies in
 155 modular tower systems.

156 Case study I analyze three different locations (Seville–Spain, Daggett–USA and
 157 Carnarvon–South Africa), which nowadays are involved in the development of STE plants
 158 with CR technology, and three receiver thermal power of 270, 390 and 500 MW_{th}. For the
 159 power block, three electrical gross output turbines –56, 78 and 100 MW_e– have been
 160 selected respectively. The heat transfer fluid used is MNS that allows working the turbine
 161 at higher temperatures (nearly 575 °C) and storing some excess energy.

162 The influence of the variation in the net electricity production and its location has been
 163 analyzed to assess the impact over the main design characteristics of the solar field and the
 164 receiver sub-systems and over the relative LEC, with respect to the reference system, on
 165 the present market.

166

167 **2.3. Case II: Technology analysis**

168 STE plants with CR technology in operation today include matured technologies and
 169 designs. Current steam receivers (PS10, PS20 –with saturated steam– and Sierra Sun
 170 Tower –with superheated steam–) are based on the well known steam boiler technology
 171 while MNS receiver (Gemasolar) has taken advantage of the knowledge about Solar Two
 172 [4, 5].

173 The thermal energy storage system for steam receivers is not well solved yet, highlighting
 174 a commercial thermal storage supply of 50 minutes of plant operation at 50% load for
 175 PS10 [6]. Moreover, direct steam technology providers have marketed their solution as a
 176 practical, cost-effective method for system without storage. For this reason, the case study
 177 II presents a comparative analysis between the two main technologies developed (direct
 178 steam *vs* molten salts) in terms of several parameters such as the relative LEC, with respect
 179 to the reference system, solar field efficiency, receiver efficiency, power block, parasitic
 180 efficiency and overall plant efficiency, without TES system, to evaluate both under similar
 181 design conditions.

182

183 **2.4. Case III: Storage analysis**

184 Commercial electricity-generating power tower plants under construction include Khi
185 Solar One in South Africa with 50 MW_e power and 2 hours of thermal energy storage [7],
186 Ivanpah Solar Electric Generating Station with 377 MW_e steam towers in California
187 (USA) and Crescent Dunes Plant in Tonopah with 110 MW_e power with 10 hours of TES
188 [8] MNS tower in Nevada (USA). Moreover, recently two important companies have
189 signed a partnership to construct and operate the two largest solar power tower in
190 California with 250 MW each one. This scenario confirms the increasing power plant size
191 trend. Molten salt power tower technology used to have large thermal energy storage as a
192 result of the lowest LEC [9]. Future direct steam power towers will likely include at least a
193 few hours of TES to increase the value of electricity produced and increase capacity factor
194 as well as dispatchability that is an important key for the grid operator, like Khi Solar One
195 in South Africa. A variety of storage options for steam systems is presented in [10].

196 Consequently, the case study III analyzes, for a given reflective surface and the two main
197 technologies (MNS and DSG system), the impact of different combinations of thermal
198 energy storage and power block sizes over the net electricity production and the relative
199 LEC, with respect to the reference system.

200

201 **2.5. Case IV: Component's cost analysis**

202 Market trends are focused on the specific cost reduction by increasing the plant size
203 through an improved economy of scale even though newer schemes are claiming the
204 economics of smaller units [11]. The cost of power tower plants can be reduced by [9]:

- 205 • Reducing equipment capital cost via reduced material content, lower-cost materials,
206 more efficient design, or less expensive manufacturing and shipping costs,
- 207 • Reducing field assembly and installation costs via simpler designs and minimization
208 and/or ease of field assembly,
- 209 • Lowering operation and maintenance costs through improved automation, reducing
210 need and better O&M techniques,
- 211 • Building larger systems that provide economies of scale,
- 212 • Deploying more systems to benefit from learning-curve effects.

213 As a result, case study IV analyze for the location of Daggett–USA three receiver thermal
214 power (270, 390, 500 MW_{th}) with the gross output power and the TES hours resulting of
215 minimizing the relative LEC in section 4.3.2, carrying out a sensitivity analysis over the
216 specific costs of major components –solar field, solar receiver, thermal storage, power
217 block, steam generator and operation and maintenance–.

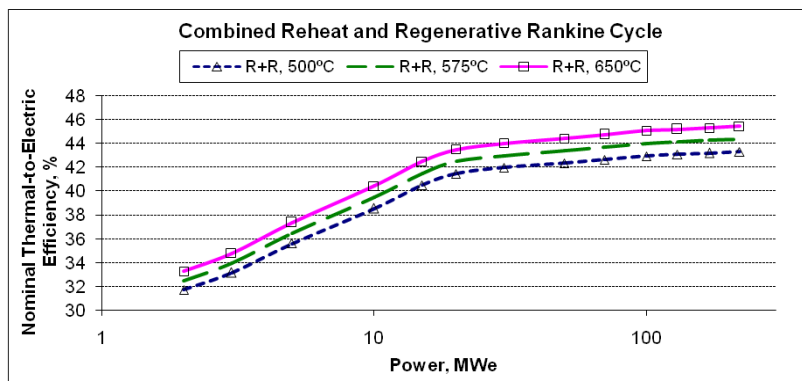
218

219 **3. General considerations**

220 *3.1. Conditions for the studies*

221 For all cases, a surround heliostat field is chosen because the Utility Studies [12-14]
222 showed that it resulted in lower LEC than a north heliostat field for large plants. The
223 115.36 m² heliostat developed for Gemasolar is selected due to its demonstrated capacity
224 to accomplish with required feasibility and profitability [15]. The optical error for the
225 heliostat is taken as 2.3 mrad RMS [16] with a mirror reflectivity assumed to be 90%.
226 Solar mirrors are available today that are 94%; this was reduced by an assumed cleanliness
227 factor of 96% [8].

228 For the turbine, a combined reheat and regenerative Rankine cycle is considered. The
229 nominal thermal-to-electric efficiency is calculated for an inlet temperature of 575 °C, an
230 inlet pressure of live steam of 100 bar, a condensing pressure of 0.04 bar and 16 °C ITD at
231 design conditions between the steam at the turbine outlet (condenser inlet) and the ambient
232 temperature. For the condenser type, an air-cooled system was chosen. Fig. 3 depicts the
233 turbine efficiency at nominal conditions for different power ranges [17]. The thermal-to-
234 electric efficiency increases rapidly for lower power ranges while achieving a plateau for
235 higher power ranges. The higher the inlet temperature is, the higher thermal-to-electric
236 efficiency will be.



237 **Fig. 3. Combined reheat and regenerative rankine cycle efficiency for various power ranges.**
238 **2-to-220 MW_e range**

239 *3.2. Computing tools for modelling, optimization and simulation.*

240 WINDELSOL 1.0 [18-20] is an adaptation of the well-known Sandia National
241 Laboratories DELSOL3 code [19,21] for Windows, in an environment with functions such
242 as user-friendly interface, optimized defined-by-coordinates heliostat field generation,
243 calculation of solar flux distribution on the absorber and graphic representation of optical
244 parameters, heliostat field array, tower and solar receiver. WINDELSOL is used to develop
245 the optical designs. The code provides the receiver dimensions, the tower height and the
246 number and optimum distribution of heliostats necessary to absorb the specific amount of
247 thermal energy into the HTF flowing through the receiver. DELSOL is an optical design
248 tool widely used for STPP with CR technology, as the design of PS-10 and PS-20
249 commercial power towers plants in southern Spain.

250 The U.S. National Renewable Energy Laboratory's SAM is a publicly available open
251 access model based on more than two decades of collaboration between NREL and the
STE industry. SAM computer code [22], which is based on the Transient System

252 Simulation program TRNSYS [23], is used to predict the annual energy production of the
253 power plant designs, as well as the evaluation of thermal losses in the receiver and sub-
254 systems and overall plant efficiencies. Using this software tool, the operation of a STPP
255 with CR technology can be simulated over a full year using TMY data [24].

256 The software tools used in this study (DELSOL, WINDELSOL and SAM) have been used
257 within previous studies of power towers [25-33]. Moreover, own tools have been used.

259 *3.3. Financing and baseline costs parameters*

260 For the evaluation of the LEC, the following costs are assumed to represent what can be
261 accomplished in early commercial plants that are currently planned or under construction
262 [8]:

- 263 • Land: 2 €/m²,
- 264 • Solar Field: 200 €/m²,
- 265 • Reference Solar Receiver: 200 €/kW_{th},
- 266 • MNS Thermal Storage: 30 €/kWh,
- 267 • PCM Thermal Storage: 50 €/kWh [34],
- 268 • Reference Power Block: 1000 €/kW_e,
- 269 • Steam Generator: 350 €/kW_e,
- 270 • Fixed Operation & Maintenance: 65 €/kW_e/y.

271
272 The cost values for the *Solar Receiver* and *Power Block + Steam Generator* are used to
273 calculate the cost of a reference design (similar to Gemasolar) and then the final cost of
274 both sub-systems are reduced through an improved economy of scale with the receiver area
275 and the gross power rating the power block respectively. The expressions are of a form
276 commonly used in chemical process industries [35]:

$$277 C_{rec} = C_{rec,ref} \left(\frac{A}{A_{rec,ref}} \right)^{x_{rec}}$$

$$278 C_{PB+SG} = C_{PB+SG,ref} \left(\frac{\eta_{th-e} \cdot P}{P_{ref}} \right)^{x_{PB+SG}}$$

279
280 LEC for the CR plants was calculated with the following according to [21, 36]:

$$281 LEC = \frac{crf \cdot K_{invest} + K_{O\wedge M} + K_{fuel}}{E_{net}}$$

282 where

$$283 crf = \frac{k_d \cdot (1 + k_d)^n}{(1 + k_d)^n - 1} + k_{insurance}$$

284 The crf is the parameter that includes all the capital-financing related assumptions in the
285 analysis. The values used in the paper are based on usual financing parameters similar to
286 that in [36], shown in Table II:

Table II. Financing parameters

Annual insurance rate	1 %
Real debt interest rate	8 %
Plant life time	30 y
Plant availability	93 %
Indirect costs	16.5 %
Construction period	2 y
Interest of investment during construction period	10.08 %
Fossil fuel backup	No
Subsidies	No

287 **4. Methodology and results**

288 **4.1. Case I: Size and location analysis**

289 The three sites selected are those involved in the implementation of STE plants with CR
290 technology. Main specifications adopted are summarized in Table III [37-38]:

Table III. Selected locations characteristics

Site	Seville Spain	Daggett USA	Carnarvon South Africa
Latitude, °	37.42	34.87	-30.97
Longitude, °	-5.9	-116.8	22.13
Altitude, m	31	588	1309
Design Point DNI, W/m ²	900	950	1000
Annual Energy DNI, kWh/(m ² ·y)	2089	2791	2995

291
292 MNS receivers have been demonstrated in pre-commercial demonstrations plants in the
293 USA at a 5 MW_{th} scale (Sandia National Laboratories) and at a 40 MW_{th} scale (Solar Two)
294 and in Europe at a 10 MW_{th} receiver tested in France (Themis) [39]. The first commercial
295 plant began operation in Spain in 2011, with Gemasolar project that uses a 120 MW_{th}
296 receiver. This paper has focused in the next generation of thermal receivers with powers
297 that ranged from 270 to 500 MW_{th} and different power productions with several hours of
298 TES.

299 The trend to reduce specific costs by increasing the plant size is partially restricted, for
300 STE with CR technology, mainly by the loss of optical efficiency due to atmospheric
301 attenuation. Moreover, higher spillages are associated to both the larger errors
302 (misalignment, wind disturbance, etc.) of the further away located heliostats and with
303 optimized receiver sizes.

304 WinDelsol [18] provides the optical design of the selected power plants. Fig. 4 shows the
305 expected field efficiencies at design point and annual performance versus the necessary
306 reflective surface (km²) for three locations and three receiver thermal powers for MNS
307 technology. Fig. 4 shows that for similar optical efficiencies, the location of Seville (Spain)
308 needs higher reflective surface to supply the necessary thermal power onto the receiver
309 whilst the location of Carnarvon (South Africa) requires the lowest reflective surface.

310

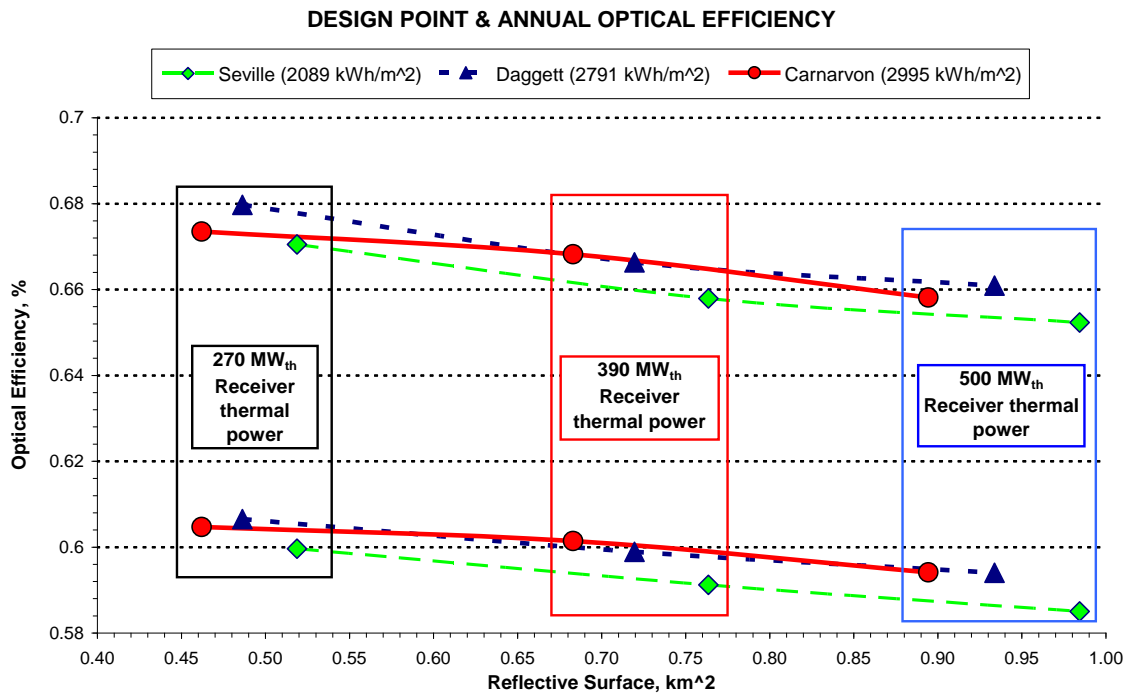


Fig. 4. Design point (upper lines) and annual optical efficiency (lower lines) vs. the reflective surface for 3 locations and 3 receiver thermal power

311 Once the field layout is optimized it is used as a new input for SAM to predict the annual
 312 energy production of the optimized power plant designs. With these results, the variation
 313 over the LEC of the optimized plant designs is analyzed.

314 Table IV presents, for three sites (Seville–Spain, Daggett–USA and Carnarvon–South
 315 Africa) and three receivers thermal power (270, 390 and 500 MW_{th}), the basic design
 316 characteristics. Furthermore, Fig. 5 depicts the relative LEC, plant investment, net annual
 317 energy and reflective surface, with respect to the reference system.

Table IV. Basic design characteristics for the nine selected cases and the reference system

Location	Reference	Seville			Daggett			Carnarvon		
		Tower height, m	140	155	180	215	150	175	200	145
Receiver surface, m ²	300	452	669	865	452	670	866	450	670	876
Receiver thermal power, MW _{th}	120	270	390	500	270	390	500	270	390	500
TES, h	15	6	7	7	7	8	8	8	9	9
Gross output power, MW _e	19.9	56	78	100	56	78	100	56	78	100

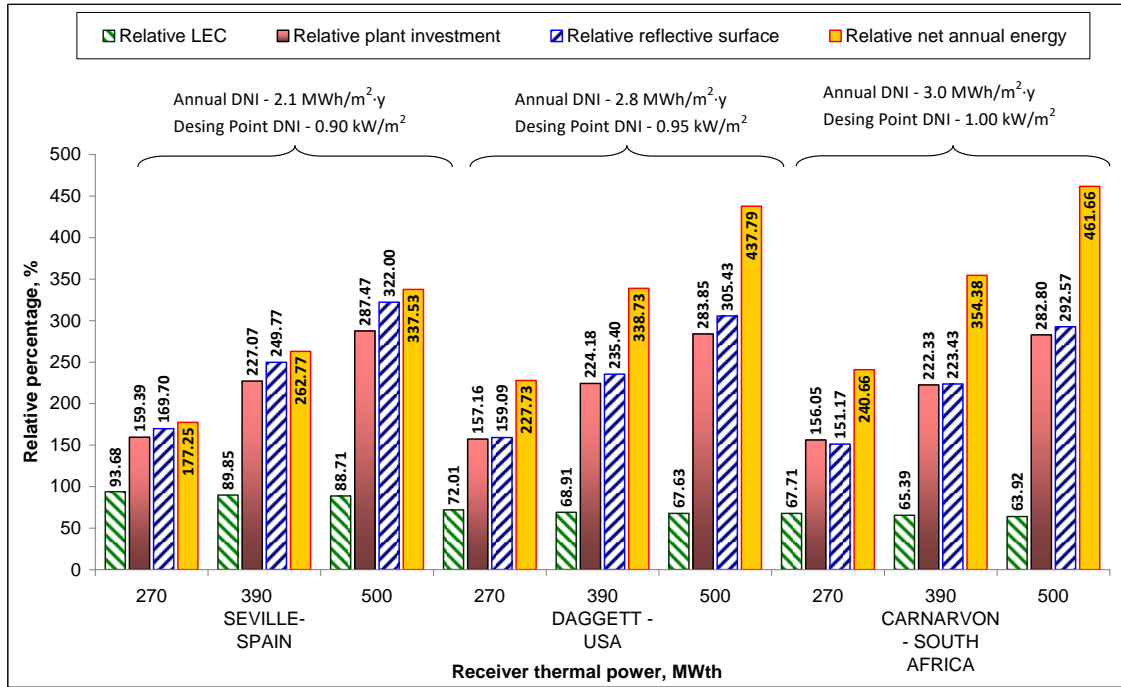


Fig. 5. Summary of the relative LEC, plant investment, net annual energy and reflective surface for the cases of Table IV

319 For the three locations, increasing the receiver thermal power means a relative LEC
 320 reduction and relative net annual energy increase. Moreover Fig. 5 depicts an almost
 321 constant relationship between the total direct plant investment and the reflective surface for
 322 all the nine cases analyzed, with an increasing of both factors by increasing the receiver
 323 thermal power of each plant.

324 Comparing the plant performance in the three locations, it can be concluded that an
 325 increase of the annual DNI entails a reduction of LEC and an increase of net annual
 326 energy, what in the cases of study of this paper means higher LEC and lower net annual
 327 energy in Seville than Daggett and Carnarvon. On the other hand, reflective surface and
 328 plant investment increase with an annual DNI decrease. The comparison for a MNS CR
 329 technology with a receiver thermal power scale-up factor of 1.9, from 270-to-500 MW_{th},
 330 presents an improvement in the LEC due to scaling up the plant of 5.3% for Seville, 6.1%
 331 for Daggett and 5.6% for Carnarvon. This LEC reduction does consider no improvement in
 332 manufacturing costs. Moreover, the analysis shows that for a similar receiver thermal
 333 power, the net annual energy could be increased around 35%, from Seville-to-Carnarvon,
 334 whilst reduces the LEC around 28%. The LEC reduction from Seville-to-Daggett is 23%.

335 With respect to the reference power tower plant (120 MW_{th}), simulated cases present a
 336 scale-up factor of the receiver thermal power between 2.3 (270 MW_{th}) to 4.2 (500 MW_{th}).
 337 Analyzing the evolution of relative LEC it can be stated that for the highest receiver
 338 thermal power (500 MW_{th}), the LEC decreases in Seville, Daggett and Carnarvon by
 339 11.3%, 32.4% and 36.1% respectively. Furthermore, it can be observed that the relative
 340 annual energy production increases with the receiver thermal power in different scale-up
 341 factor depending on the annual DNI. Therefore, it is noticeable that the relative annual
 342 energy production scale-up factor is lower, similar and higher in Seville, Daggett and
 343 Carnarvon respectively (Table V).

Table V. Scale-up factors comparison with respect to the reference plant

Receiver thermal power scale-up factor	2.3	3.3	4.2	
Net annual production scale-up factor	Seville	1.8	2.6	3.4
	Daggett	2.3	3.4	4.4
	Carnarvon	2.4	3.5	4.6

344 4.2. Case II: *Technology analysis*

345 Although it is widely assumed that any molten salt receiver would have accompanying
346 with thermal energy storage, since this is a key benefit of the MNS concept, direct steam
347 technology providers have marketed their solution as a practical, cost-effective method for
348 system without storage. As a result, the present section is focused on the analysis of the
349 differences between MNS and DSG technologies without TES while section 4.3 would
350 analyze in depth the different options for the TES for both technologies.

351 The performance of a MNS without thermal storage is similar to a parabolic trough power
352 plant which has a buffer tank that absorbs oil changes. In this particular case, a drainage
353 tank is considered to store the salts during transients or night periods.

354 For the design of both DSG and MNS plants the following assumptions have been made:

- 355 • The location of Seville is selected for the analysis,
- 356 • Thermodynamic conditions adopted for the steam going to the power block are the
357 same in both technologies,
- 358 • The same electrical gross output is delivered (111 MW_e),
- 359 • The solar field/receiver has been designed for a maximum solar flux over the
360 receiver of ~1 MW/m² [8] for MNS technology and for the DSG the maximum
361 solar flux is sub-divided as function of the type of receiver. For the boiler the
362 maximum solar flux is ~0.8 MW/m², for the super-heater is ~0.5 MW/m² and for
363 the re-heater is ~350 kW/m² [22],
- 364 • The tower height is set to 170 m.

365 DSG consists of superheated steam at 575°C and 100 bars that feeds the high pressure
366 turbine. The receiver includes a re-heater where a portion from the high pressure turbine
367 outlet is redirected and reaches a temperature of 500°C and then passes through the
368 remainder of the power cycle. MNS outlet temperature from the receiver is 580°C, and
369 produces steam at 575°C and 100 bar.

370 With respect to the parasitic, common losses have been considered for both technologies:
371 heliostat, piping, auxiliary heater, and self-supply. And, in the case of MNS additional
372 losses due to the necessity of pumping the HTF through the heat exchanger and through
373 the drainage tank; And the necessity of maintaining the salt temperature during transient
374 and night periods as well as the system preheating on start-up.

375 First, an analysis for different solar multiples (ratio of the thermal power that is absorbed in
376 the receiver fluid and delivered to the base of the tower at the system design point to the
377 peak thermal power required by the turbine-generator [21]) is carried out, to find out the
378 one that minimized the relative LEC and/or maximizes the relative overall plant efficiency.

379 Fig. 6 depicts the solar multiple optimization for both power plants without thermal energy
380 storage. The LEC calculation, for the DSG system, has neglected the cost related to the
381 steam generator.

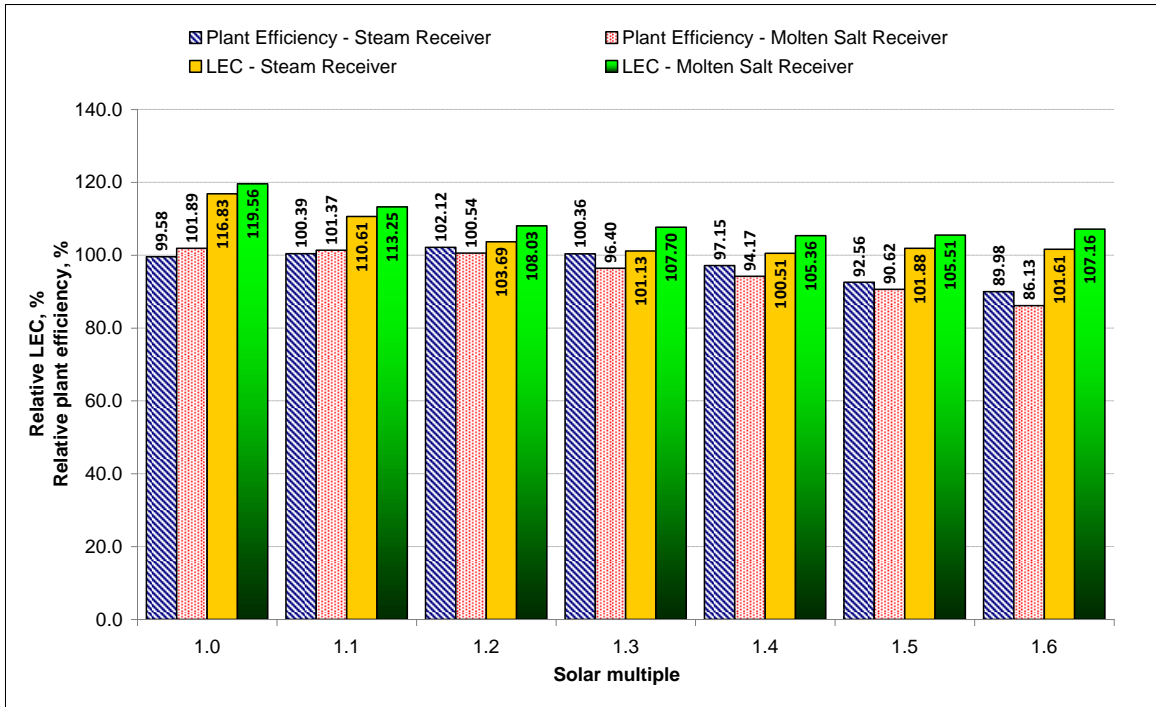


Fig. 6. Solar multiple optimization as function of the relative LEC – plant efficiency for a MNS and DSG system

382

383 The results depicts that, for the DSG technology, the solar multiple which maximizes the
 384 plant efficiency is 1.2 while the solar multiple that minimizes the LEC is 1.4. For the MNS
 385 technology, the solar multiple which maximizes the plant efficiency is 1.0 while the solar
 386 multiple that minimizes the LEC is 1.4.

387 Second, as a result of Fig. 6, Table VI shows the basic design characteristics and
 388 efficiencies for a solar multiple of 1.1 at which, both technologies have similar relative
 389 plant efficiency and relative LEC.

**Table VI. Characteristics and efficiencies for for a DSG and a MNS power tower
 with a solar multiple of 1.1.**

¹ Net annual energy for a plant availability of 100 %

Solar Multiple	1.1	
Technology	DSG	MNS
Receiver thermal power, MW _{th}	277.8	277.8
Receiver surface, m ²	724	471
Heliosstat number, -	4574	4645
Total convective losses, GWh/y	54.77	22.56
Total radiative losses, GWh/y	20.31	23.16
Solar field annual efficiency, %	51.95	50.38
Receiver annual efficiency, %	80.89	80.26
Power block annual efficiency, %	38.88	41.26

Parasitic efficiency, %	91.40	90.66
Net electric output ¹ , GWh	164.7	168.9
Relative LEC, %	110.61	113.25
Plant efficiency, %	14.93	15.08

390

391 The solar field efficiency is 1.6% higher for DSG mainly because the spillages for a larger
392 area are lower.

393 Furthermore, the worse heat transfer for water/steam compared with MNS causes that the
394 flux working ranges are lower for the first ones (Table VII). This involves that the
395 necessary surface for the heat transfer mechanisms is larger so the convective losses of a
396 DSG are larger than just the increase due to the larger surface. However, the efficiencies of
397 both receivers are quite similar for this solar multiple.

Table VII. Flux ranges of solar tower receivers

Fluid	Water/Steam	MNS
Flux, kW/m ²		
- Average	100 – 300	400 – 500
- Peak	400 – 800	700 – 1000

398

399 As the MNS plant presents shorter starting-up and shutdown times compared with heated
400 steam plants and, at the same time, transients have a better behaviour on MNS plant, power
401 cycle works more time a year in nominal conditions for MNS plant maximizing the
402 efficiency of the plant and decreasing LEC. This fact is even more impacting taking into
403 account storage: in this case, power cycle is decoupled from the solar radiation, eliminating
404 transients on the turbine and reducing turbine starting-up time.

405 The total parasitic losses are higher for the MNS system than for the DSG. Besides the
406 heliostat, the piping and the auxiliary heater losses for both technologies, the MNS system
407 includes the required pumping power for the HTF through the power block; which means
408 higher parasitic losses for a power tower with MNS than for a power tower with DSG.

409 The minimum relative LEC for a DSG power plant is 100.51 % for a solar multiple of 1.4
410 while the minimum relative LEC for a MNS power plant is 105.36 % for a solar multiple
411 of 1.4. The variation is within 1.1 c€/kWh.

412 As a conclusion it can be stated that, for a power tower without thermal energy storage and
413 with the same thermodynamic requirements for the power block, a DSG system results in a
414 lower LEC than a MNS system and a similar LEC than the reference plant with 15 hours of
415 TES. Previous studies confirm this prediction [9].

416

417 **4.3. Case III: Storage analysis**

418 TES increases the value of the electricity produced. That the reason why MNS power
419 tower plants include large TES. On the other hand, TES for DSG is under intensive
420 research to achieve competitive values. The main options for both technologies are:

- 421 a) MNS: TES for molten nitrate salt technology is based on the active direct storage
422 systems [40]. It consists of two tanks, the hot tank to store the HTF coming from the
423 receiver, in order to use it during cloudy periods or nights. The cold tank where the
424 cooled HTF remains waiting to be heated. Fig. 1 depicts a schematic view of the
425 reference system, that uses molten nitrate salts as HTF.
- 426 b) DSG: TES for direct steam generation technology is based or in an active direct
427 storage system or in a combination of an active indirect and passive storage system
428 [40]. The first option, direct storage of saturated or superheated steam in pressure
429 vessels, is not economic due to the low volumetric energy density [41]. The second
430 type has three different storage options under investigation [34]. All of them uses
431 PCM storage for evaporation/condensation storage [42]. The main changes in the
432 configuration are mainly due to the sensible part with the usage of concrete [42] or
433 molten salts storage. A storage system with a capacity of approximately 1MWh
434 working at 100 bar was constructed by DLR combining a PCM module and a concrete
435 module. The storage modules have been tested in a DSG-test facility specially erected
436 at a conventional power plant of Endesa in Carboneras (Spain) [42].

437 Case III analyzes, for the two main CR technologies, (MNS and DSG), different
438 combinations of TES and power block sizes over the net electricity production and relative
439 LEC.

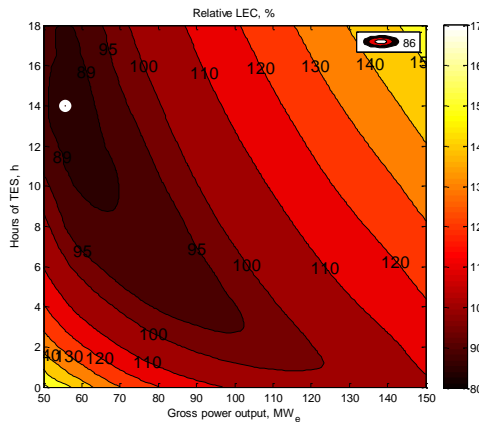
440 Previous studies have compared a reference technology with DSG with TES using PCM
441 storage [34] or have analyzed a DSG with a theoretical TES system [43] for parabolic
442 trough technology. For the analysis presented in this work, it has been considered the
443 thermal behaviour of a theoretical thermal storage system [44], with a charging/discharge
444 utilization factor and a global efficiency of 85% [45]. This value is applied in accordance
445 with [46] that established the annual thermal storage efficiencies for Solar One and CESAs-
446 1 power plant, CR systems with DSG, 83 % and 84 % respectively.

447 For the design of both DSG and MNS plants the following assumptions have been made:

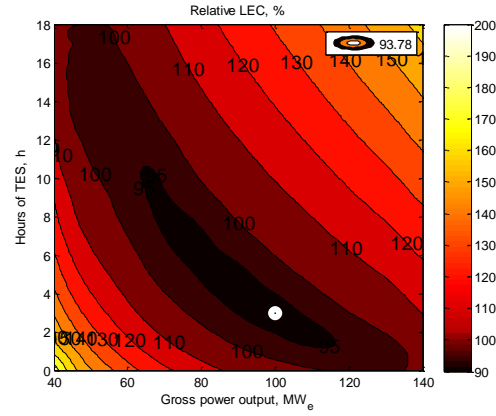
- 448 • Three locations (Table III) and three receiver thermal power (270, 390 and 500
449 MW_{th}) are analyzed,
- 450 • Thermodynamic conditions adopted for the steam going to the power block are the
451 same in both technologies,
- 452 • The same electrical gross output is delivered (33-to-167 gross output MW_e) with a
453 variation of TES hours (0-to-18),
- 454 • The solar field has been designed for a maximum solar flux over the receiver of ~ 1
455 MW/m^2 [8] for MNS technology and for the DSG the maximum solar flux is sub-
456 divided as function of the type of receiver. For the boiler the maximum solar flux is
457 $\sim 0.8 MW/m^2$, for the super-heater is $\sim 0.5 MW/m^2$ and for the re-heater is ~ 350
458 kW/m^2 [22],
- 459 • The same criteria adopted for the HTF in section 4.2 are adopted in this section.

460 The design criteria used for most of conventional and renewable power plants is the
 461 minimization of the electricity cost, LEC, for STPP. Therefore, Fig. 7 and Fig. 8 shows a
 462 detailed analysis about different combinations of TES (0-18 hours) and gross power output
 463 sizes (33-156 MW_e) over relative LEC, for a MNS and a DSG power plant respectively, in
 464 Seville, as an example of the methodology followed for the cases presented below. This
 465 location is selected because of its importance in the development of STPP with CR
 466 technology. With respect to the thermal power, it is also selected a receiver of 390 MW_{th},
 467 corresponding to a scale-up factor of 3.3 respect to Gemasolar and 9.8 respect to Solar
 468 Two, as the intermediate step towards the envisaged 1000 MW_{th} capacity [8].

469



470
 471 **Fig. 7. Relative LEC for different combinations**
 472 **of TES and gross power output for a 390 MW_{th}**
 473 **receiver with MNS technology and 0.76 km²**
 474 **reflective surface in Seville**



475
 476 **Fig. 8 Relative LEC for different combinations**
 477 **of TES and gross power output for a 390 MW_{th}**
 478 **receiver with DSG technology and 0.76 km²**
 479 **reflective surface in Seville**

480 For a receiver thermal power of 390 MW_{th} located in Seville, the analysis carried out for
 481 both technologies depicts:

- 482 • MNS: The minimum relative LEC occurs for a gross power output of 55.5 MW_e
 483 with 14 hours of TES with a relative LEC of 86.0%. The corresponding net electric
 484 generation is 251.3 GWh with an overall plant efficiency of 14.65%,
- 485 • DSG: The minimum relative LEC occurs for a gross power output of 100 MW_e
 486 with 3 hours of TES with a relative LEC of 93.8%. The corresponding net electric
 487 generation is 250.0 GWh with an overall plant efficiency of 14.62%.

488 For this particular case (390 MW_{th} in Seville), all the combinations of TES and gross
 489 power output, for DSG and MNS, have been presented in Fig. 7 and Fig. 8. Hereafter, the
 490 following sub-sections will present, using the same methodology, the minimum relative
 491 LEC, the corresponding TES hours and net electricity production for the aforementioned
 492 cases.

493

494

495

496

488 **4.3.1. Seville – Spain**

489 In accordance with the stated conditions in 4.3., Fig. 9 presents for both CR technologies,
 490 MNS and DSG, the minimization results for the relative LEC. The total reflective surface
 491 of the solar field is presented in the legend.

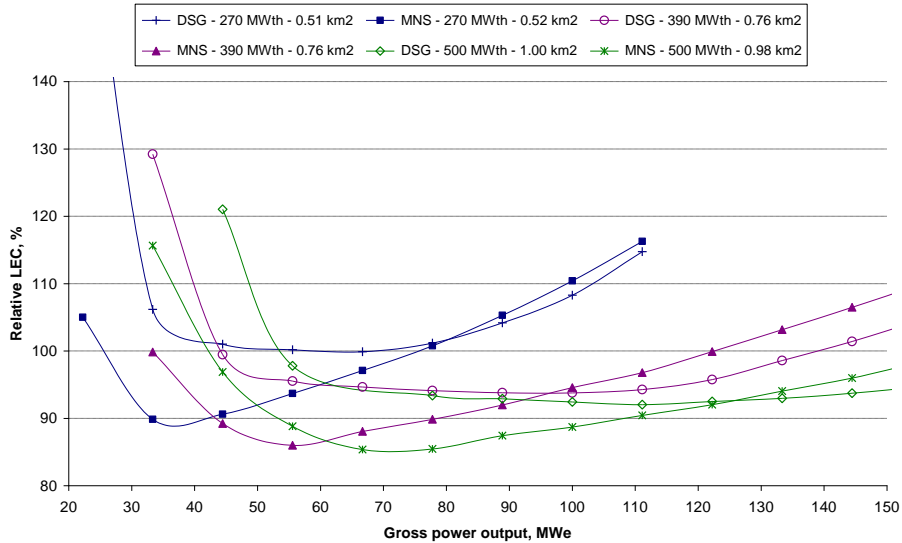


Fig. 9. Relative LEC minimization for different combinations of TES and power block sizes, for MNS and DSG technology, in Seville-Spain

492 Fig. 10 depicts the TES hours that minimizes the relative LEC of Fig. 9, for different gross
 493 turbines powers (22-to-166 MW_e) and TES hours (0-to-18 hours). This figure shows that
 494 both technologies minimize the relative LEC for the same TES hours in almost all the
 495 cases studied.

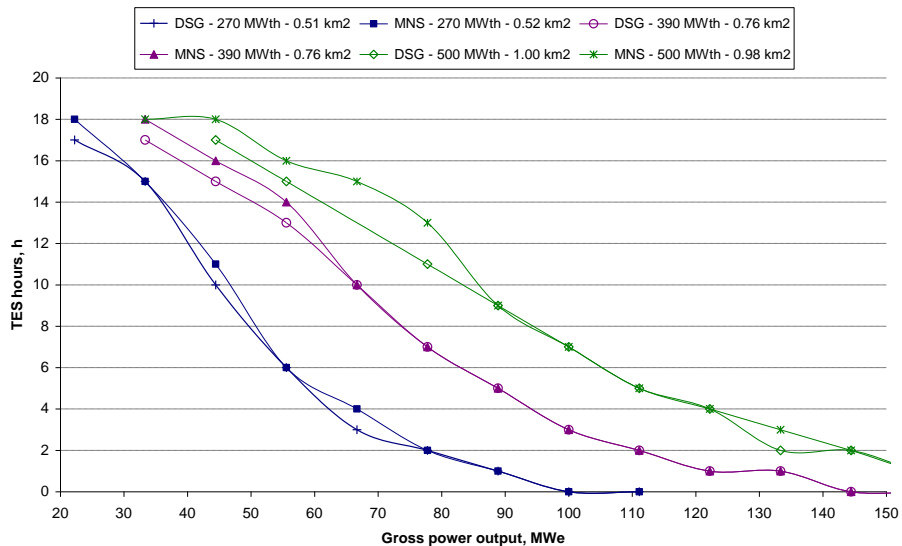


Fig. 10. TES hours that minimizes the relative LEC for different combinations of TES and power block sizes, for MNS and DSG technology, in Seville-Spain

496 Fig. 11 shows the net annual energy that minimizes the relative LEC for a MNS and a DSG
 497 CR technology. This figure presents an increasing net annual energy, depending on the

498 receiver thermal power, until achieving a plateau for a turbine power that minimizes the
 499 LEC, with the TES hours presented in Fig. 10.

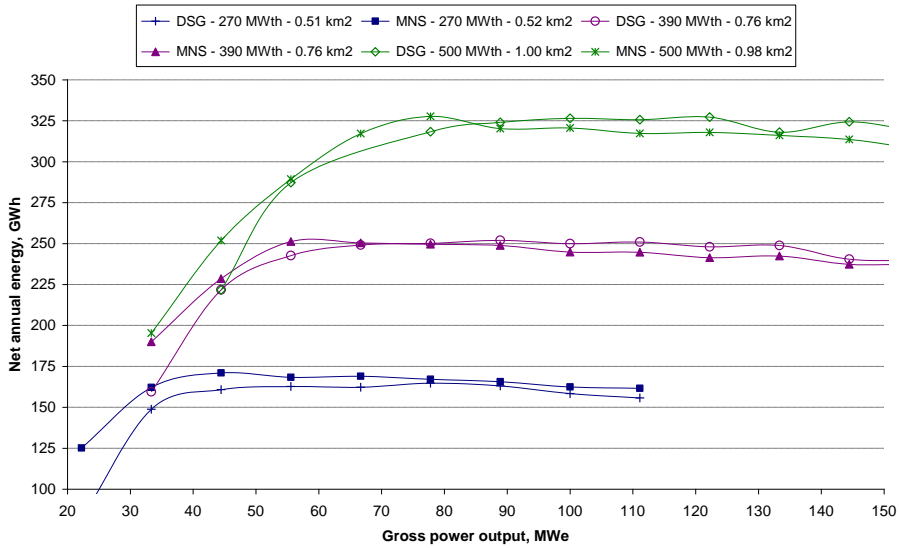


Fig. 11. Net annual energy that minimizes the relative LEC for different combinations of TES and power block sizes, for MNS and DSG technology, in Seville-Spain (100% plant availability)

500 Table VIII and Table IX summarizes the parameters that minimized the relative LEC for
 501 each receiver thermal power for both technologies.

502

503 4.3.2. Daggett – USA

504 In accordance with the stated conditions in 4.3., Fig. 12 presents for both CR technologies,
 505 MNS and DSG, the minimization results for the relative LEC. The total reflective surface
 506 of the solar field is presented in the legend.

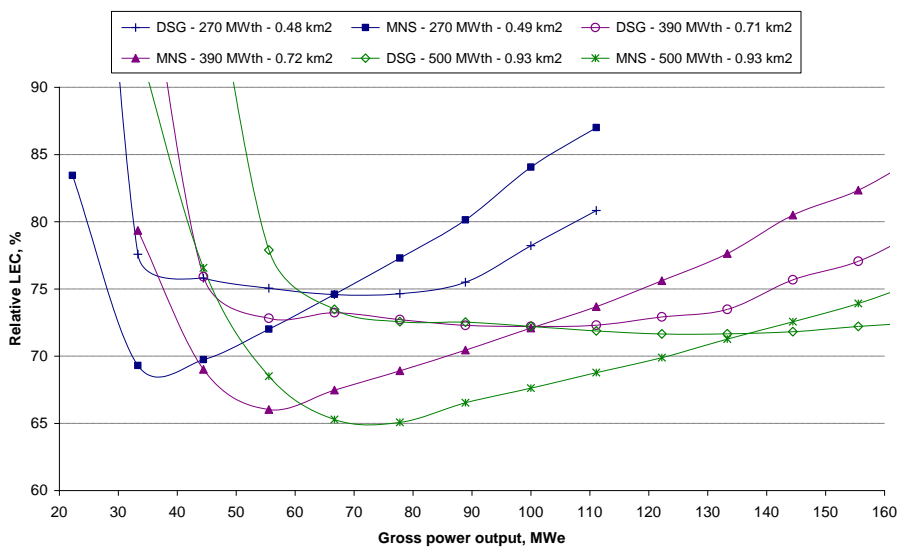


Fig. 12. Relative LEC minimization for different combinations of TES and power block sizes, for MNS and DSG technology, in Daggett-USA

507 Fig. 13 depicts the TES hours that minimizes the relative LEC of Fig. 12 for different gross
 508 turbines powers (22-to-166 MW_e) and TES hours (0-to-18 hours). This figure shows that
 509 DSG usually requires less TES hours than MNS technology to minimize the relative LEC.

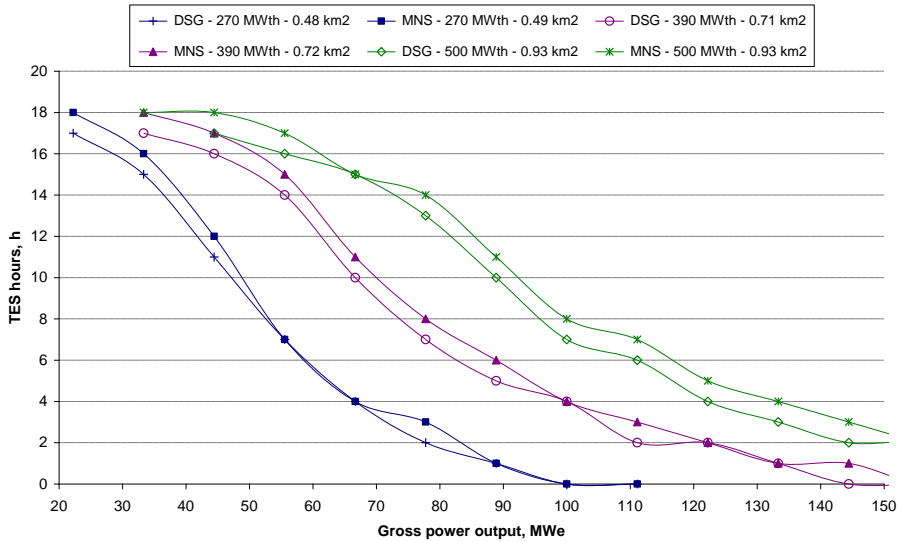


Fig. 13. TES hours that minimizes the relative LEC for different combinations of TES and power block sizes, for MNS and DSG technology, in Daggett-USA

510 Fig. 14 shows the net annual energy that minimizes the relative LEC for a MNS and a DSG
 511 CR technology. This figure presents the same behavior of Fig. 11.

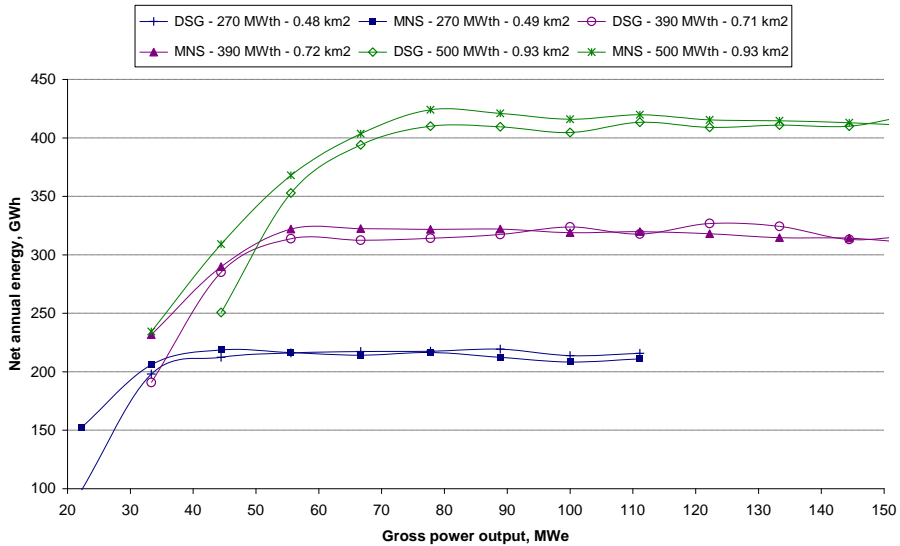


Fig. 14. Net annual energy that minimizes the relative LEC for different combinations of TES and power block sizes, for MNS and DSG technology, in Daggett-USA(100% plant availability)

512 Table VIII and Table IX summarizes the parameters that minimized the relative LEC for
 513 each receiver thermal power for both technologies.

514

515

516 **4.3.3. Carnarvon – South Africa**

517 In accordance with the stated conditions in 4.3., Fig. 15 presents for both CR technologies,
 518 MNS and DSG, the minimization results for the relative LEC. The total reflective surface
 519 of the solar field is presented in the legend.

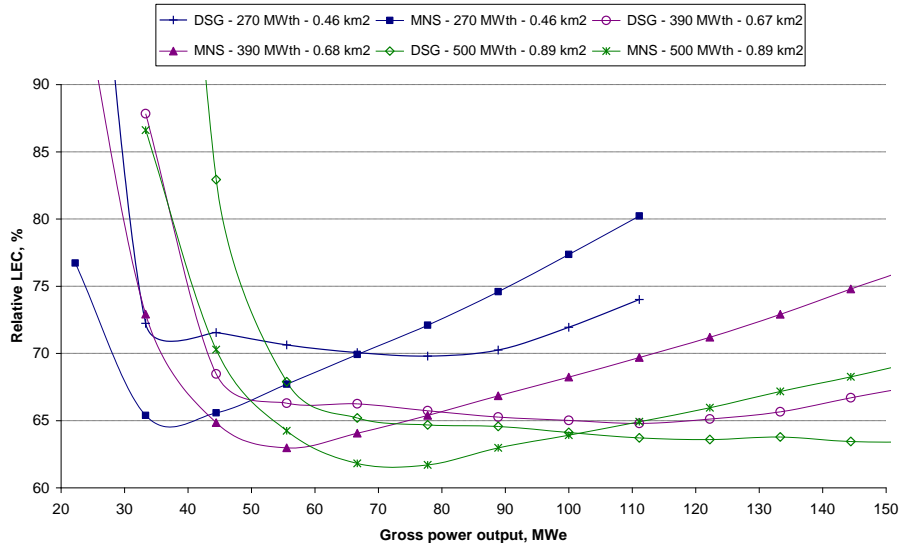


Fig. 15. Relative LEC minimization for different combinations of TES and power block sizes, for MNS and DSG technology, in Carnarvon – South Africa

520 Fig. 16 depicts the TES hours that minimize the relative LEC of Fig. 15 for different gross
 521 turbines powers (22-to-166 MW_e) and TES hours (0-to-18 hours). This figure shows that
 522 DSG usually requires 2 hours less than MNS technology to minimize the relative LEC.

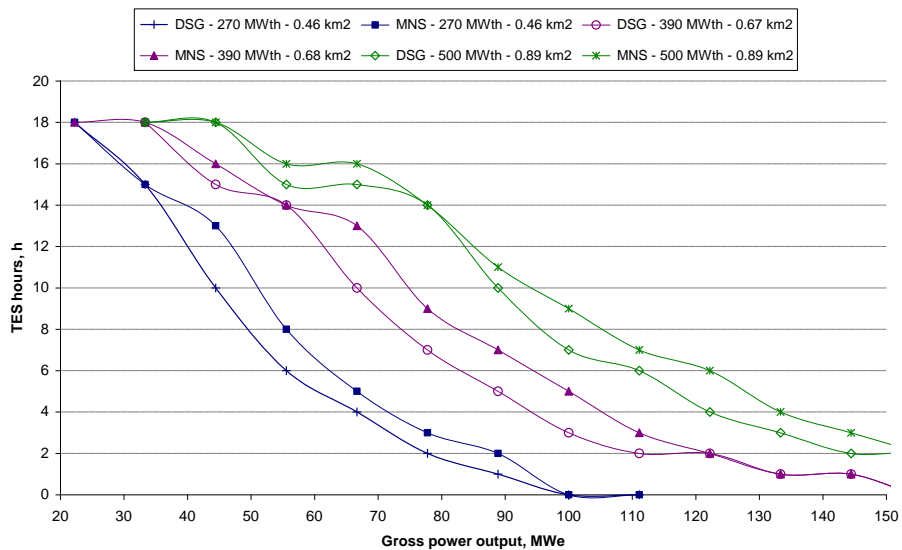


Fig. 16. TES hours that minimizes the relative LEC for different combinations of TES and power block sizes, for MNS and DSG technology, in Carnarvon – South Africa

523 Fig. 17 shows the net annual energy that minimizes the LEC for a MNS and a DSG CR
 524 technology. This figure presents the same behavior of Fig. 11 and Fig. 14.

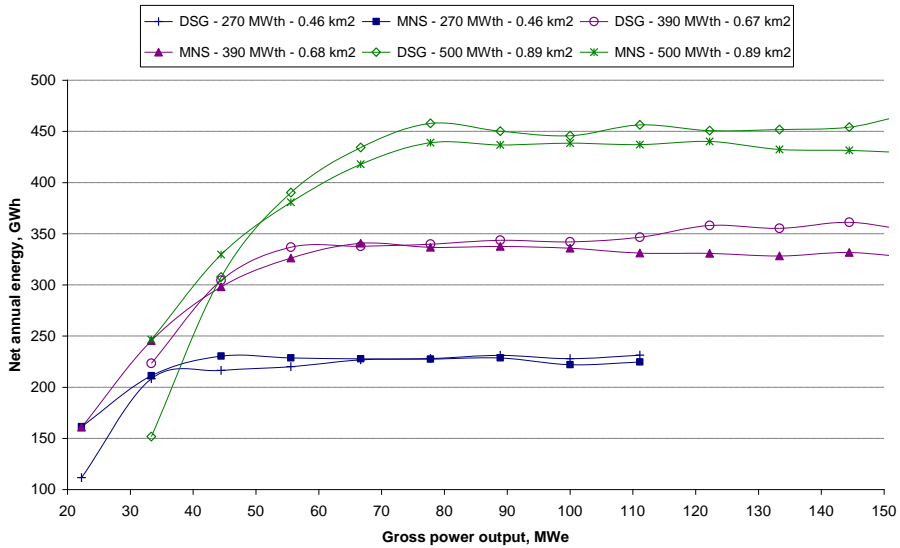


Fig. 17. Net annual energy that minimizes the relative LEC for different combinations of TES and power block sizes, for MNS and DSG technology, in Carnarvon – South Africa (100% plant availability)

525 Table VIII and Table IX summarizes the parameters that minimized the relative LEC for
 526 each receiver thermal power for both technologies.

527 Both technologies demonstrate, despite the location, that larger plants achieve lower LEC
 528 regardless of the technology.

Table VIII. Summary of basic parameters to minimize relative LEC for MNS

Location	Seville – Spain			Daggett – USA			Carnarvon – South Africa		
Receiver thermal power, MW _{th}	270	390	500	270	390	500	270	390	500
Relative LEC, %	89.9	86.0	85.4	69.3	66.0	65.1	65.4	63	61.7
Gross power output, MW _e	33	56	67	33	56	78	33	56	78
TES, h	15	14	15	16	15	14	15	14	14

Table IX. Summary of basic parameters to minimize relative LEC for DSG

Location	Seville – Spain			Daggett – USA			Carnarvon – South Africa		
Receiver thermal power, MW _{th}	270	390	500	270	390	500	270	390	500
Relative LEC, %	99.9	93.8	92.0	74.6	72.2	71.7	69.8	64.8	63.6
Gross power output, MW _e	67	100	111	67	100	122	78	111	122
TES, h	3	3	5	4	4	4	2	2	4

529

530 The outcomes (Table VIII-Table IX) reveal two main tendencies due to the importance of
 531 the thermal energy storage. MNS technology offers commercial, cost-efficient, and
 532 competitive storage system. As a result, for a receiver thermal power, the minimization of
 533 the relative LEC appears for low values of gross turbine power output but very high TES.
 534 This phenomenon, permits to work the turbine at design point conditions longer periods.

535 On the other hand, DSG technology provide theoretical/pre-commercial, high cost-less
 536 efficient (estimated 85% [45-46]) storage. With these assumptions, for a receiver thermal

537 power, the minimization of the relative LEC occurs for high values of gross turbine power
538 output but with low values of TES.

539 The importance of the location is clearly remarkable. For STPP which nowadays are not
540 competitive with fossil fuel power plants, the development and construction of this CR
541 efficient technology in countries of the solar belt with very high annual DNI as Carnarvon
542 in South Africa (2995 kWh/m²/y) and Daggett in United States (2791 kWh/m²/y) would
543 produce a relative LEC reduction of around 38% and 35% respectively for a MNS power
544 plant. This LEC reduction combined with improvements in manufacturing and a more
545 mature power tower industry (section 4.4) would make STTP with CR technology
546 competitive in near future.

547

548 **4.4. Case IV: Component's cost analysis**

549 This study offers a component's cost analysis having into account the following
550 assumptions:

551 • The location of Daggett is selected for the analysis because of its importance in the
552 development of STPP with CR technology,

553 • Three receiver thermal power (270, 390 and 500 MW_{th}) are analyzed,

554 • The net annual energy is that obtained for the selected location in section 4.3.2,

555 • It has been used the consensus values of costs presented in Table X, that are
556 believed to be plausible due to the improvements in manufacturing, a more mature
557 power tower industry and an improved economy of scale.

558

Table X. Costs assumed to be applicable for future generation power plants [9]:

Land	2 €/m ²
Solar Field	120 €/m ²
Reference Solar Receiver	170 €/kW _{th}
MNS Thermal Storage	25 €/kWh
PCM Thermal Storage	30 €/kWh [36]
Reference Power Block	800 €/kW _e
Steam Generator	250 €/kW _e
Fixed Operation & Maintenance	50 €/kW _e /y

559

560 The results of this analysis are presented in the following sub-sections which describe
561 different aspects related to relative LEC tendencies and cost reduction associated to the
562 advances obtained in industry. The analysis is applied to the three cases for both DSG and
563 MNS that minimize the relative LEC in Daggett for each receiver thermal power in section
564 4.3.2.

565

566 **4.4.1. Relative LEC tendencies**

567 Fig. 18 depicts the impact of the expected costs goals over the relative LEC for the
568 reference power tower plant and for three power tower plants with MNS and DSG
569 technology.

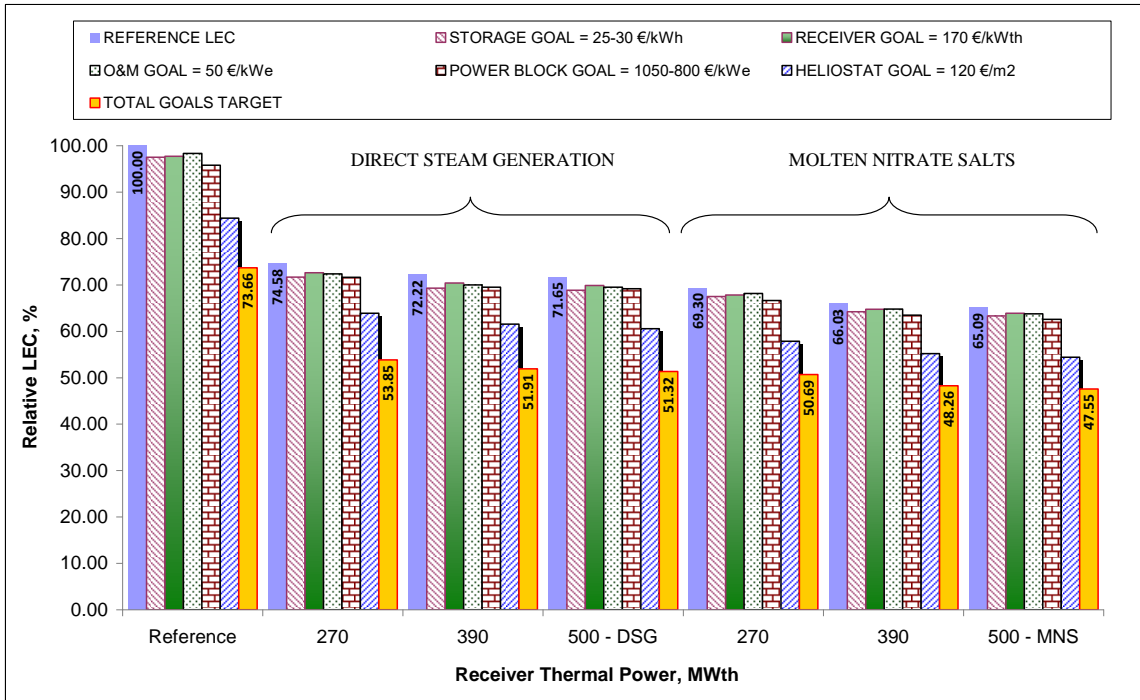


Fig. 18. Relative LEC for different sub-systems improvements over a STPP with MNS and DSG technology in Daggett

570

571 Nowadays, the relative LEC in Daggett for:

572 - DSG varies between 74.58% (270 MW_{th}) to 71.65% (500 MW_{th}) that can be
 573 reduced to 53.85% (270 MW_{th}) – 51.32% (500 MW_{th}),
 574 - MNS varies between 69.30% (270 MW_{th}) to 65.09% (500 MW_{th}) that can be
 575 reduced to 50.69% (270 MW_{th}) – 47.55% (500 MW_{th}).

576 Fig. 18 shows the huge cost reduction potential that STPP with CR technology still has to
 577 go. A MNS system, located in Daggett, with 500 MW_{th} thermal receiver that accomplish
 578 with the cost that is assumed to be plausible in near future will reduce its cost by 52%,
 579 compare to the reference plant. For a DSG 500 MW_{th} thermal receiver, that reduction will
 580 be near a 49%. This would mean that STPP with CR technology could become an
 581 important source on the energy market without necessity of subsidies at all.

582

583 4.4.2. Cost reduction

584 Fig. 19 presents the impact of the different sub-systems analyzed over the LEC reduction.
 585 For this analysis a receiver thermal power of 500 MW_{th} is selected for both technologies.

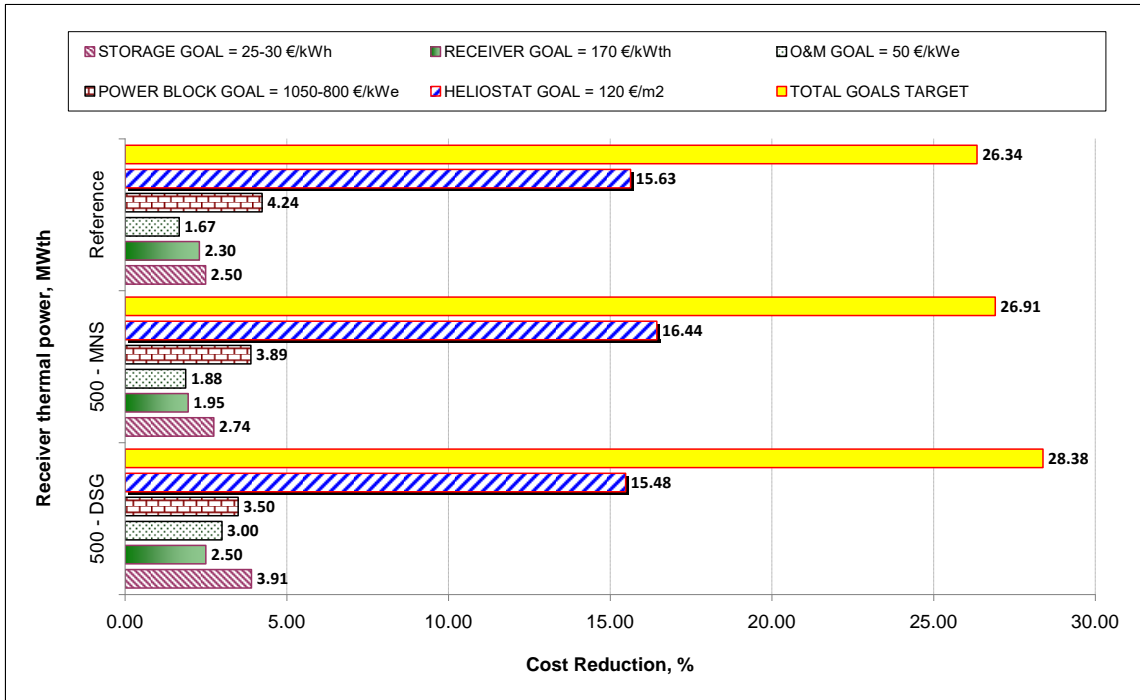


Fig. 19. Cost reduction for different sub-systems improvements over a STPP with MNS and DSG technology in Daggett

586

587 Fig. 19 shows that the higher LEC reduction (15-to-16%) is produced by the solar field.
 588 Moreover, O&M costs are related to the plant size, in such a way that the higher the power
 589 plant size is, the higher LEC reduction is expected. For a DSG system, the reduction due to
 590 the TES (3.9%) is much more important than for the MNS technology (2.7%). For the
 591 other sub-systems, the relative improvement is quite similar. The maximum LEC reduction
 592 after the combination of all the improvements is in between 25-to-30%. This target is
 593 expected to be achievable in future generation power plants with the assumptions
 594 considered in the analysis.

595 The cost reduction produced by the different sub-systems is quite similar for the three
 596 locations and receiver thermal power.

597

598 **5. Conclusions**

599 The paper presents an analysis for a medium to large size (290-to-500 MW_{th} receiver
600 thermal power) CR plant considering the present market trends. The study is separated in
601 four sub-sections:

602 - Size and location analysis: the main countries, nowadays, involved in the development
603 of power tower plants are Spain, USA and South Africa. Therefore, this analysis was
604 focused in three locations of these countries: Seville, Daggett and Carnarvon
605 respectively. The comparison for a MNS CR technology with a receiver thermal
606 power from 270 to 500 MW_{th}, presents an improvement in the LEC due to scale up the
607 plant of 5.3% for Seville, 6.1% for Daggett and 5.6% for Carnarvon. Moreover, the
608 analysis shows that for a similar power plant design, the net annual energy could be
609 increased around 35%, from Seville-to-Carnarvon, whilst reduces the LEC around
610 28%. The LEC reduction from Seville-to-Daggett is 23%.

611 With respect to the reference power tower plant (120 MW_{th}), this paper presents a
612 scale-up factor of between 2.3-to-4.2. The relative LEC for a 500 MW_{th} receiver
613 decreases for Seville, Daggett and Carnarvon by 11.3%, 32.4% and 36.1%
614 respectively.

615 - Technology analysis: direct steam technology providers have marketed their solution
616 as a practical, cost-effective method for system without storage. Therefore, in this sub-
617 section the main technologies (DSG and MNS) without TES have been studied. It was
618 concluded that a DSG system results in a lower LEC (100.51%) than a MNS system
619 and a similar LEC (105.36 %) than the reference plant with 15 hours of TES (100%).
620 Previous studies confirm this prediction [9].

621 - Storage analysis: when designing a thermal power tower plant, an important issue is to
622 make the decision about the power of the turbine and the size of the thermal energy
623 storage, once the receiver thermal power is selected. Consequently, this sub-section
624 has simulated, for the two main technologies (MNS and DSG systems) and for the
625 three selected locations (Seville, Daggett, Carnarvon), the impact of different
626 combinations of thermal energy storage and power block sizes over relative LEC, for
627 each optimized power plant.

628 The outcomes reveal two main tendencies due to the importance of the thermal energy
629 storage. MNS technology minimizes the relative LEC for low values of gross turbine
630 power (33 to 78 MWe) and very high TES (14 to 16 hours). On the other hand,
631 considering the difficulties to find out real information about TES costs for DSG, the
632 LEC analysis has been carried out using the assumptions made in section 3.3 (PCM
633 thermal energy storage: 50 €/kWh [34]). As a result, the relative LEC obtains its
634 minimum value at high values of gross turbine power (67 to 122 MWe) and at low
635 values of TES (2 to 5 hours).

636 - Component's cost analysis: market trends are focused on the specific cost reduction by
637 means of larger plant size and through an improved economy of scale. Based on
638 baseline cost parameters widely accepted in solar industry, an analysis over the
639 specific costs of major components on the electricity cost has been carried out. For the
640 analysis, the location of Daggett has been selected. The analysis was applied to the
641 three cases for both DSG and MNS that minimized the relative LEC in Daggett for
642 each receiver thermal power in section 4.3.2.

643 A MNS system, located in Daggett, with 500 MW_{th} thermal receiver that accomplish
644 with the cost that are assumed to be plausible in near future will reduce the relative
645 LEC by 52%, compared to the reference plant. A DSG with 500 MW_{th} thermal
646 receiver the reduction will be near a 49%.

647 The higher LEC reduction is produced by the solar field sub-system by a 15-to-16%.
648 For a DSG system, the reduction due to the TES (3.9%) is much more important than
649 for the MNS technology (2.7%). For the other sub-systems, the relative improvement
650 is quite similar. The maximum LEC reduction after the combination of all the
651 improvements is in between 25-to-30%. This target is expected to be achievable in
652 future generation power plants with the assumptions considered in the analysis.

653
654 Finally it can be concluded that this paper summarizes a variety of options for STPP with
655 CR working with MNS and DSG. Nowadays these system are not competitive with fossil
656 fuel power plants, but the research, development and construction of this CR efficient
657 technology in countries of the solar belt with very high annual DNI as Carnarvon in South
658 Africa (2995 kWh/m²/y) and Daggett in United States (2791 kWh/m²/y) would produce a
659 relative LEC reduction of around 38% and 35% respectively. Furthermore, the
660 combination of sunny countries, as Spain, with the improvements in manufacturing and a
661 more mature power tower industry would make STTP with CR technology competitive in
662 near future conducting to a LEC reduction due to these improvements of up to a 30%.

663
664

665 **Acknowledgements**

666 The author wish to thank “Comunidad de Madrid” and “European Social Fund” for its
667 financial support to the SOLGEMAC Project through the Programme of Activities
668 between Research Groups (S2009/ENE-1617). The author wishes to acknowledge Ms.
669 M.A. Martinez Tarifa for her many helpful comments.

670 **References**

- 671 [1] Richter, C., Teske, S., Nebrera, J.A., Concentrating Solar Power – Global Outlook
672 2009, Greenpeace, SolarPaces and ESTELA 2009
- 673 [2] Medrano M, Gil A, Martorell I, Potau X, Cabeza LF., “State of the art on high
674 temperature thermal energy storage for power generation. Part 2 – case studies”,
675 Renewable and Sustainable Energy Reviews, Volume 14, Issue 1, January 2010, Pages
676 56-72.
- 677 [3] Garcia, E, and Calvo, R., “One year operation experience of Gemasolar plant”,
678 SolarPACES 2012, Marrakech, Morocco, September.
- 679 [4] H. E. Reilly and G. J. Kolb, “Evaluation of Molten Salt Power Tower Technology
680 Based on Experience at Solar Two”, SAND2001-3674. Sandia National Laboratories,
681 Albuquerque, NM, November 2001.
- 682 [5] J. E. Pacheco (editor), “Final Test and Evaluation Results from the Solar Two Project”,
683 SAND2002-0120. Sandia National Laboratories, Albuquerque, NM, January 2002.
- 684 [6] Romero M., Zarza E., “Concentrating Solar Thermal Power”. In Handbook of Energy
685 Efficiency and Renewable Energy. F. Kreith and Y. Goswami (Eds.) Chapter 21. 2007,
686 pp. 1-98. CRC Press Taylor & Francis Group, Boca Raton, Florida.
- 687 [7] Renewable energy country attractiveness indices, Ernst & Young, 2012, Issue 32,
688 available online, accessed November 2012: <http://www.ey.com/>
- 689 [8] Kolb G.J., “An Evaluation of Possible Next Generation High Temperature Molten Salt
690 Power Towers”, 2011, Report No. SAND2011-9320.
- 691 [9] Kolb G.J., Ho C.K., Mancini T.R. and Gary J.A., “Power Tower Technology Roadmap
692 and Cost Reduction Plan”, 2011, Report No. SAND2011-2419.
- 693 [10] Laquil III D, Schafer C.T. and Faas S. E., “A Cost-Performance Comparison of Water
694 Steam Receivers for Solar Central Electric Power Plants”, December, 1980, SAND80-
695 8245.
- 696 [11] Romero M., et al, “Distributed power from solar tower systems: A MIUS approach”,
697 Solar Energy, 2000, Issue 67 (4-6), pp. 249-264.
- 698 [12] Pacific Gas & Electric Company, “Solar Central Receiver Technology Advancement
699 for Electric Utility Applications, Phase 1 Topical Report”, 1988, Report No. 007.2-88.2,
700 San Francisco, CA.
- 701 [13] Arizona Public Service Company, “Utility Solar Central Receiver Study”, 1988,
702 Report No. DOE/AL/38741-1.
- 703 [14] Alternate Utility Team, “Utility Solar Central Receiver Study”, 1988, Report No.
704 DOE/AL/38741-2.
- 705 [15] Lata J., Alcalde S., Fernandez D., Lekube X., “First surrounding field of heliostats in
706 the world for commercial solar power plants - Gemasolar”. Proceedings SolarPACES,
707 2010, Perpignan, France.
- 708 [16] A. B. Zavoico, “Solar Power Tower Design Basis Document”, Rev. 0, SAND2001-
709 2100. Sandia National Laboratories, Albuquerque, NM, July 2001.
- 710 [17] Biencinto M., Personal communication, Plataforma Solar de Almeria, 2010.

711 [18] AICIA, CIEMAT, SOLUCAR Central Receiver Technologies. “WinDelsol 1.0 Users
712 Guide”, 2002, Spain.

713 [19] Garcia, P., Ferriere, A., Bezian, J.J., “Codes for solar flux calculation dedicated to
714 central receiver system applications: A comparative review”, Solar Energy, 2008, Vol.
715 82, pp. 189–197.

716 [20] Fernandez, V., Silva, M., Romero, M., WinDelsol 1.0. In: Pitz-Paal, R. (Ed.), Proc. Of
717 the 15th Task III Meeting within IEA SolarPACES on Solar Technology and
718 Applications, Cologne, Germany, 2001, June 19, SolarPACES Tech. Report. DLR,
719 Koln, Germany.

720 [21] Kistler B.L., “A User's Manual for DELSOL3-A Computer Code for Calculating the
721 Optical Performance and Optimal System Design for Solar Thermal Central Receiver
722 Plants”, 1986, SAND86-8018.

723 [22] Gilman, P., et al., Solar Advisor Model User Guide for Version 2.0, National
724 Renewable Energy Laboratory Technical Report NREL/TP-670-43704, August 2008
725 (www.nrel.gov/analysis/sam/).

726 [23] TESS, 2011. <<http://www.trnsys.com/>>, 11/8/11, Thermal Energy System Specialists,
727 LLC (T.E.S.S.), Madison Wisconsin.

728 [24] NREL, 1961, <http://rredc.nrel.gov/solar/old_data/nsrdb/1961-1990/tmy2/>, 2/6/12,
729 National Renewable Energy Laboratory, Golden, Colorado.

730 [25] Teichel, S.H., Feierabend, L., Klein, S.A., Reindl D.T, “An alternative method for
731 calculation of semi-gray radiation heat transfer in solar central cavity receivers”, Solar
732 Energy, 2012, Vol. 86, p. 1899–1909.

733 [26] Wagner, S.J., Rubin, E.S, “Economic implications of thermal energy storage for
734 concentrated solar thermal power”, Renewable Energy, 2012,
735 <http://dx.doi.org/10.1016/j.renene.2012.08.013>.

736 [27] Abbas, M. Boumeddane, B., Said, N., Chikouche, A, “Dish Stirling technology: A
737 100 MW solar power plant using hydrogen for Algeria”, International journal of
738 hydrogen energy, 36, 2011, p.4305-4314.

739 [28] Thevenard, D., Pelland, S, “Estimating the uncertainty in long-term photovoltaic yield
740 predictions”, Sol. Energy, 2011, doi:10.1016/j.solener.2011.05.006.

741 [29] Romero, M., and Gonzalez-Aguilar, J., “Multitower Solar Thermal Power Plants With
742 Heliostat Fields: An Assessment Of Optical And Thermal Efficiency”, SolarPACES
743 2011, Granada, Spain, September.

744 [30] Kribus, A., Zaibel, R., Carey, D., Segal, A., and Karni, J., “A Solar-driven Combined
745 cycle power plant”, Solar Energy, 1998, Vol. 62, No. 2, pp. 121–129.

746 [31] Montes, M.J., Rovira, A., Martínez-Val, J.M., and Ramos, A., “Proposal of a fluid
747 flow layout to improve the heat transfer in the active absorber surface of solar central
748 cavity receivers”, Applied Thermal Engineering, 2012, Vol. 35, pp.220-232.

749 [32] Sanchez, M. and Romero, M., “Methodology for generation of heliostat field layout in
750 central receiver systems based on yearly normalized energy surfaces”, Solar Energy,
751 2006, Vol. 80, pp. 861–874.

752 [33] Noone, C.J., Torrilhon, M., Mitsos, A., “Heliostat field optimization: A new
753 computationally efficient model and biomimetic layout”, Solar Energy, 2012, Vol. 86
754 pp. 792–803.

755 [34] Feldhoff JF, Schmitz K, Eck M, Schnatbaum-Laumann L, Laing D, Ortiz-Vives F,
756 Schulte-Fischbeck J, “Comparative system analysis of direct steam generation and
757 synthetic oil parabolic trough power plants with integrated thermal storage”, Solar
758 Energy, Volume 86, Issue 1, January 2012, Pages 520-530.

759 [35] Guthrie K.M., “Capital Cost Estimating”, Chemical Engineering, 1969, pp. 114-142.

760 [36] Pitz-Paal R., et al., “Development steps for concentrating solar power technologies
761 with maximum impact on cost reduction”. Proceedings of ISEC 2005, Florida.
762 [37] Venter, N., Netshilaphala, N., “Environmental Impact Assessment Process. Proposed
763 Concentrating Solar Power (STE) Plant and Associated Infrastructure in the Northern
764 Cape Area”, 2006. Available online, accessed November 2012:
765 http://www.eskom.co.za/content/BID_Final_English230306.pdf
766 [38] Meyer, A., Niekerk, J.L., “Roadmap for the deployment of concentrating solar power
767 in South Africa”, SolarPACES 2011, Granada, Spain, September.
768 [39] Ho, C.K. and Iverson, B.D, “Review of Central Receiver Designs for High-
769 Temperature Power Cycles”, SolarPACES 2012, Marrakech, Morocco, September 11-
770 14.
771 [40] Gil A, Medrano M, Martorell I, Lázaro A, Dolado P, Zalba B, Cabeza LF., “State of
772 the art on high temperature thermal energy storage for power generation. Part 1-
773 Concepts, materials and modellization”, Renewable and Sustainable Energy Reviews,
774 Volume 14, Issue 1, January 2010, Pages 31-55
775 [41] Steinmann WD, Eck M, “Buffer storage for direct steam generation”, Solar Energy,
776 Volume 80, Issue 10, October 2006, Pages 1277-1282.
777 [42] Laing D, Bahl C, Bauer T, Lehmann D, Steinmann WD, “Thermal energy storage for
778 direct steam generation”, Solar Energy, Volume 85, Issue 4, April 2011, Pages 627-633
779 [43] Montes, M.J., Abanades A., Martinez-Val J.M., “Performance of a direct steam
780 generation solar thermal power plant for electricity production as a function of the solar
781 multiple”. Solar Energy 2009;83:679-89.
782 [44] Winter, C.J. et al., “Solar Power Plants: Fundamentals, Technology, Systems,
783 Economics”. Springer-Verlag, Berlin, 1990, pp. 199–214.
784 [45] Montes, M.J., “Análisis y propuestas de sistemas solares de alta exergía que emplean
785 agua como fluido calorífero”. Madrid, 2008; Ph.D. Dissertation, Universidad
786 Politécnica de Madrid.
787 [46] Baker, A.F. et al., “U.S.- Spain Joint Evaluation of the Solar One and CESA-I
788 Receiver and Storage Systems”, 1989, Report No. SAND88-8262, SNL, Alburquerque,
789 NM. EEUU.
790